REPORT/PAPER, THESIS, or DISSERTATION
as a partial requirement
for
the course on

Laser Metrology and Non-Destructive Testing

ME5304 C Term 2025

Verification of NACA-4197 algorithm for composite rocket fins using Scanning Laser Doppler Vibrometry

Submitted by:

Reya Truher

Reya Truher

Partners: David Strom

David Strom

Submitted to:

Professor Cosme Furlong-Vazquez

NEST – NanoEngineering, Science, and Technology
CHSLT- Center for Holographic Studies and Laser micro-mechaTronics
Mechanical Engineering Department
School of Engineering
Worcester Polytechnic Institute
Worcester, MA 01609-2280

3/8/2025

Summary

The goal of this project is to prove that the NACA-4197 method of analyzing fin flutter is accurate to composite materials using Scanning Laser Doppler Vibrometry (SLDV). The motive for this project comes from aeroelastic flutter, which is one of the main causes of fin failure in rocketry. Aeroelastic flutter, especially within fiberglass composite fins, is difficult to measure using traditional methods as these fins are often handmade and are inconsistent. As such, this project will be using Scanning Laser Doppler Vibrometry, allowing for high precision measurements of the vibrational modes of the fins.

Acknowledgements

We would like to express our gratitude to Professor Cosme Furlong-Vazquez for his guidance and expertise throughout this project. Additionally, we extend our thanks to his PHD students, in particular Danny Ruiz-Cadalso and Howard Zheng, as they were extremely helpful in setting up and troubleshooting the equipment. We also are grateful and extend thanks to WPI's Center for Holographic Studies and Laser micro-mechatronics for providing access to the necessary facilities and equipment. Lastly, we appreciate the support from our colleagues who provided valuable feedback and assistance during the research process.

Table of Contents

Verification of NACA-4197 algorithm for composite rocket fins using Scanning Laser Doppler Vibrometry

List of Figures

List of Tables

Nomenclature

FFT	Fast Fourier Transform, a mathematical technique for transforming signals from time to frequency domain
FFF	Fully Finished Fin, a test sample with full composite layering on both sides
HFF	Half Finished Fin, a test sample with partial composite layering
NACA	National Advisory Committee for Aeronautics, the predecessor to NASA
PSV	Polytec Scanning Vibrometer, a system used for non-contact vibration measurements
RTD	Real-Time Data, indicating measurements collected and analyzed in real time
SIM FG	Simulated Fiberglass Fin, a computational model of a fully fiberglass fin
SIM WOOD	Simulated Wood Fin, a computational model of a wooden fin
SLDV	Scanning Laser Doppler Vibrometry, a non-contact technique for measuring vibration and velocity
UFF	Unfinished Fin, a test sample with only a base material layer

1.0 Introduction

One of the primary causes of failure in fin-stabilized rockets is a phenomenon called “fin flutter”. This occurs when the fins are excited at a frequency close to their torsional resonant frequency, causing increasing displacement and eventually structural failure. Fin flutter is also a historically difficult phenomenon to analyze. The two foundational texts on the subject are NACA-TN-685 and NACA-TN-4197, both National Advisory Committee for Aeronautics (NACA) technical notes from the mid-20th century. The former is an analysis of experimental data only, deriving equations solely from wind tunnel data. The latter is a purely theoretical exploration, using physical relations between fin shape and material properties to provide a low fidelity but simple method of calculating fin flutter velocity. This limited analysis does not provide for anisotropic materials such as fiberglass, which is commonly used in modern rockets. In this paper, we will explore the use of a Polytec Scanning Laser Doppler Vibrometer in combination with the NACA-685 algorithm to attempt to verify the NACA-4197 algorithm for use with composite fin materials.

2.0 Methods

This section will explain both mathematical background and our methodology behind the structure of the project.

2.1 NACA TN 4197

Published by the National Advisory Committee for Aeronautics (NACA) in 1958, NACA Technical Note 4197, titled "Summary of Flutter Experiences as a Guide to the Preliminary Design of Lifting Surfaces on Missiles," is a technical report authored by Dennis J. Martin. This document provides research into various fin flutter phenomena in the design of missile systems. This paper provided much insight into the cause of fin flutter, and it also provided various equations to calculate fin flutter. The equations in TN 4197 are intended to provide a fast method of approximating the flutter velocity. While this may not be as accurate as an in-depth analysis, it allows for rapid iteration when designing a system. The most relevant of these equations being shown below in figure 1 to solve for the fin flutter velocity with respect to the speed of sound of a lifting surface, such as a rocket fin or an aircraft wing [1].

$$\left(\frac{V_f}{a}\right)^2 = \frac{G_E}{\frac{39.3A^3}{\left(\frac{t}{c}\right)^3(A+2)}\left(\frac{\lambda+1}{2}\right)\left(\frac{p}{p_0}\right)}$$

[1]

Figure 1: Fin flutter velocity equation from NACA TN 4197 [1]

This equation solves for the fin flutter velocity of a specific lifting surface, V_f, where,

1. $a =$ The speed of sound
2. $G_E =$ The shear modulus of the fin material
3. $\frac{t}{c} =$ The thickness-to-chord ratio (represents the relative thickness of the fin airfoil section)
4. $A =$ The aspect ratio of the fin (ratio of fin span to its mean aerodynamic chord)
5. $\lambda =$ The taper ratio (ratio of the tip chord length to the root chord length)
6. $\frac{p}{p_0} =$ The pressure ratio (ratio of ambient pressure to sea-level standard atmospheric pressure, used to adjust for altitude effects)
7. $39.3 =$ Empirical constant derived from experimental data in NACA TN 4197

2.2 NACA TR 685

NACA TN 4197 also references an additional paper titled NACA TR 685. In this report, a relationship where the ratio of the first bending mode and first tortional mode resonant frequency values relate to the ratio of the flutter frequency and the first tortional frequency. As this technical report is a purely experimental one, many of the relations given are in the form of graphs and lines of constant variable [3]. In this case, there are four graphs corresponding to different physical parameters of the wing, and there are lines of constant x_a plotted. This relationship can be seen in figure 2 below, where:

1. $\omega_h$is the first bending frequency
2. ω_α is the first tortional frequency
3. ω_f is the flutter frequency

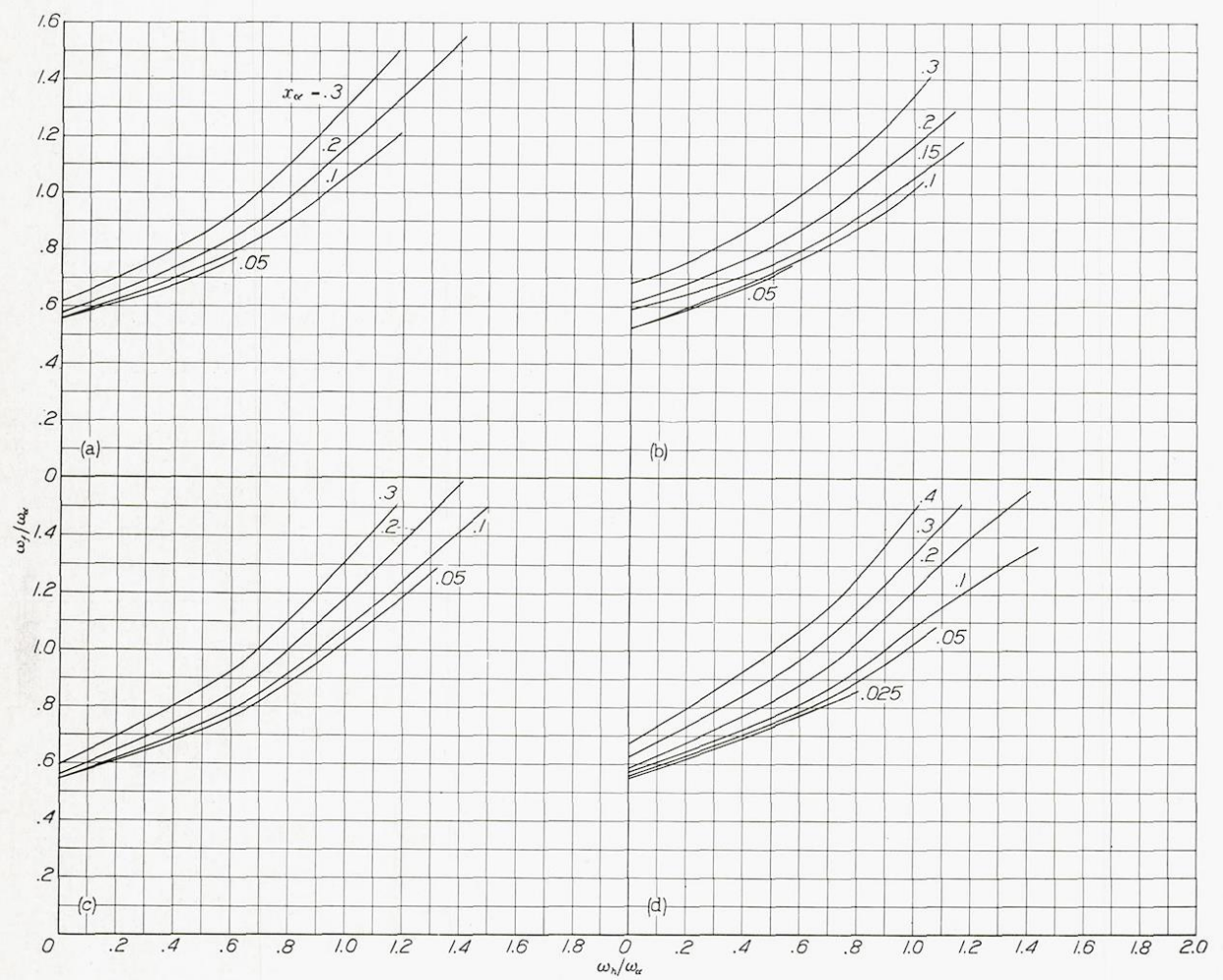

(a) $\kappa=\frac{1}{5}$; $a=-0.4$. (b) $\kappa=\frac{1}{5}$; $a=-0.2$.
(c) $\kappa=\frac{1}{10}$; $a=-0.4$. (d) $\kappa=\frac{1}{10}$; $a=-0.2$.

Graph I–F (a–d).—Flutter frequency ratio as dependent on x_α against frequency ratio; $r_\alpha^2=\frac{1}{4}$. Case 1 (h, α).

Figure 2: Four graphs of $\frac{\omega_f}{\omega_\alpha}$ vs. $\frac{\omega_h}{\omega_\alpha}$ for different κ , a , and x_a values from NACA TN 685 [3]

The measured values of our sample are:

1. $\kappa \approx \frac{1}{4}$, the wing density
2. $a \approx -0.5$, the fractional location of the neutral axis
3. $x_a \approx 0.3$, the fractional location of the center of gravity in front of the neutral axis

Thus, graph a, with the values of $\kappa \approx \frac{1}{5}$, $a \approx -0.4$ and $x_a \approx 0.3$ as seen in figure X, best matches the values for our application. Additionally, NACA TN 685 mentions the following equations to help solve for the flutter velocity based on the above parameters [3].

$$X = \frac{{r_\alpha}^2}{\kappa} * \left(\frac{\omega_\alpha}{\omega}\right)^2 \quad (1)$$

$$v = \frac{r_\alpha \omega_\alpha b}{\sqrt{\kappa}} * \frac{1}{k} * \frac{1}{\sqrt{X}} \quad (2)$$

Where:

1. v is the flutter velocity
2. r_α is the radius of gyration about the aerodynamic center
3. b is the semichord length of the fin (half of the total chord length)
4. κ is the ratio of a mass of a cylinder of air equal to the chord of the wing to the mass of the wing
5. k is the reduced frequency as defined by $k = \frac{\omega b}{V}$ where,
    a. ω is the oscillation frequency
    b. V is the free stream velocity

Therefore, if we can experimentally gather the values of $\omega_h$and ω_α, we can calculate the flutter frequency, ω_f. This can then be used in the above equation to calculate the flutter velocity. This way, we can compare our measured results with those of NACA TN 4197 and ANSYS simulations.

2.3 Scanning Laser Doppler Vibrometry

To measure the $\omega_h$and ω_α of our fin sample, a scanning laser doppler vibrometer (SLDV) was used as it offers high-precision and non-contact measurements. This allowed us to capture the modal response of composite rocket fins without interfering with their natural motion. This allows us to ensure that our data is not only accurate, but the SLDV PSV software also provides useful visuals to verify mode shapes [2].

An SLDV operates on the principle of the doppler effect, in which vibrations in an object that a laser bounces off changes the laser light in both frequency and phase. As seen in figure 3 shown below, a laser is split into a measurement beam and a reference beam, both with a frequency f_0. Then, most often using a Bragg cell, the frequency of the measurement beam is changed by a fixed frequency f_b. Next, the beam bounces off the measurement object (in this case the rocket fins), and by the doppler effect, shifts its frequency by an additional f_d. Lastly, the beams are recombined and directed towards an optical sensor in which a value f_{beat} is measured. This measured f_{beat} relates to f_d in the equation shown below with the known value of f_b [2]:

$$f_{beat} = f_d - f_b \tag{3}$$

Then, the velocity in terms of time, $v(t)$, and the position in terms of time, $x(t)$, can be solved for in the equations shown below.

$$v(t) = \frac{\lambda f_d \cos(\alpha)}{2} \tag{4}$$

$$x(t) = \int_0^t v(\tau) d\tau \tag{5}$$

Where,

1. λ is the wavelength
2. α is the angle between the measurement surface plane and the beam direction. For our experiment, as seen in the experimental setup section, the SLDV is positioned straight on to the measurement surface. Therefore, α is assumed to be $90°$, though it may vary by a few degrees as it measures points not at the center of the fin. This effect is both negligible and taken into account when setting the focus of the SLDV.

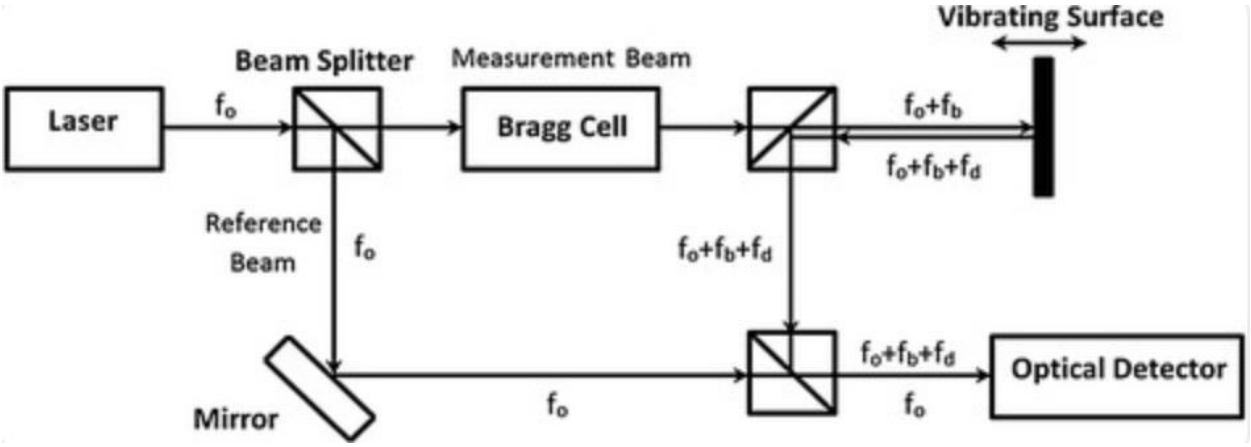

Figure 3: Visual representation of an SLDV setup [2]

3.0 Experimental Setup

The following section will explain the setup for our experiment and how our data was collected.

3.1 Physical Setup

In order to gather frequency data, the fin can both needs to be secured to the table and needs to be induced with various frequencies. We decided to use a piezoelectric shaker to induce this vibration throughout the fin can as it's able to vibrate the whole can at once. As seen in the diagram in figure 4 shown below as well as the image of the experimental setup in figure 5, the shaker is secured between two plates using screws. The bottom plate is then secured to the table while the top plate connected to threaded rods that run through the fin can. These rods screw into a bar at the top that provides a clamping force to the fin can. This design was chosen as it both secures the fin can while mimicking the vibrations the fin can would experience during rocket flight. Additionally, the SLDV was positioned at the same level and as straight on as possible to the measured fin as to have α be as close to 90° as possible.

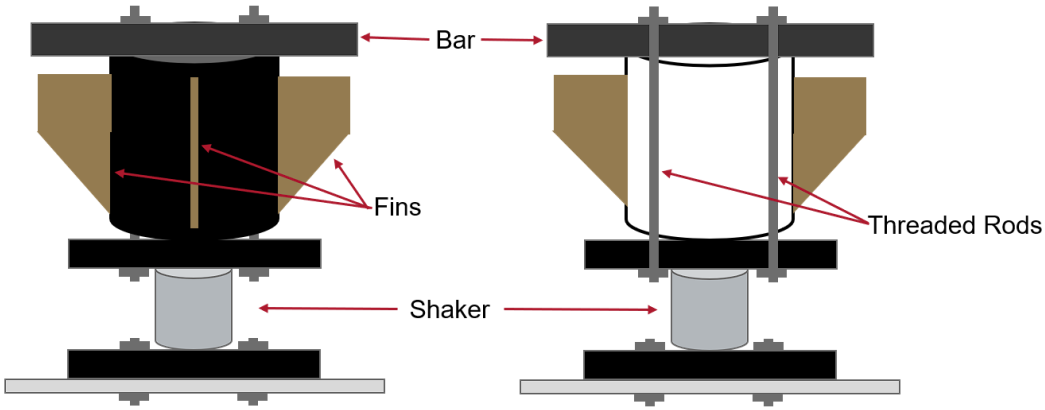

Figure 4: Diagram representing how the fin can was secured for the experiment

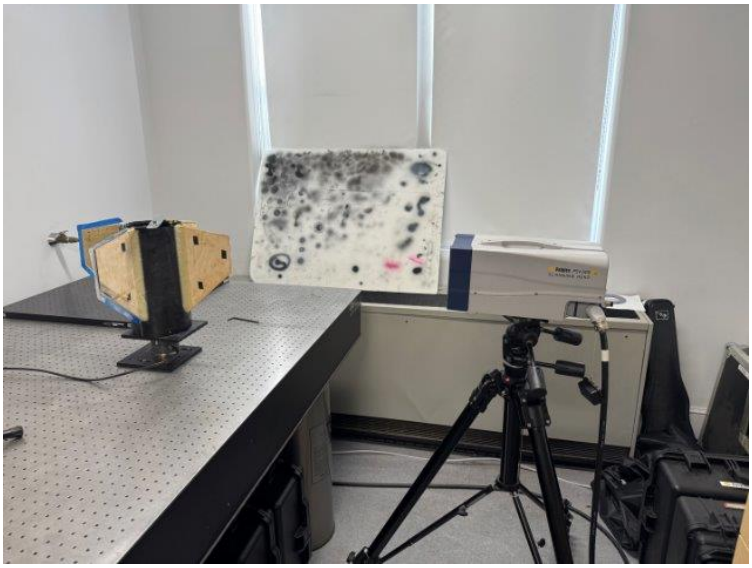

Figure 5: Photo of experimental setup

3.2 Calibration and Mesh Generation

Once the fin can and SLDV were positioned, the calibration could begin. Firstly, as seen in figure 6 below on the left, various points on the fin were selected and the SLDV was focused on each point. As it is a flat surface, as long as there are many points relatively evenly spread across the fin, the focusing shouldn't be a problem and our data should be accurate. This allowed a focus map to be used by the SLDV to know how to focus when measuring. Additionally, in the same figure on the right, the fin profile was outlined, and a mesh was generated. This mesh had 1028 points to ensure that our results were accurate. Additionally, the internal points are randomly spread throughout the fin profile using the PSV software's mesh generator tool. This means that these points don't create a pattern within the fin profile. The same mesh, though with refocused focus points, was used for each test.

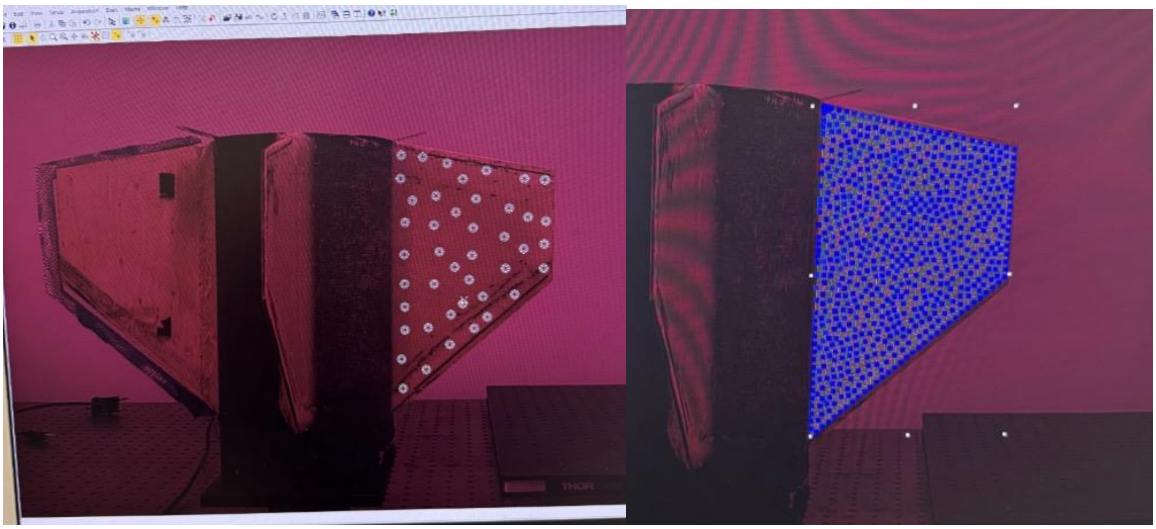

Figure 6: Focus points on fin (left) and generated fin mesh (right)

3.3 Test Settings and Result Format

We then ran a Fast Fourier Transform (FFT) scan from 1 Hz – 800 Hz as this is where our preliminary tests and benchmark data expected the mode shapes to occur. We also incorporated 3-point averaging at each point. This means that the piezoelectric shaker would sweep from 1Hz to 800 Hz while the SLDV measured the velocity and position of the fin at each point. The SLDV would scan each point three times and average the plots. This way, our data would give us an accurate depiction of the vibration at each frequency and point.

The PSV output includes a plot of the vibrational magnitude in respect to frequency as seen for each fin in figures 7, 8, and 9 below. Additionally, the software provides the motion of the fin in the form of an animated mesh. As the bending modes will always occur at a vibrational peak, we were able to go through each peak and identify which vibrational mode occurred. To visualize what we were looking for, the animations for the first bending, second bending, and first torsional modes for the fully finished fin can be seen below in figures 10, 11, and 12 (Unfortunately, the animations don’t play in .pdf but should in .docx).

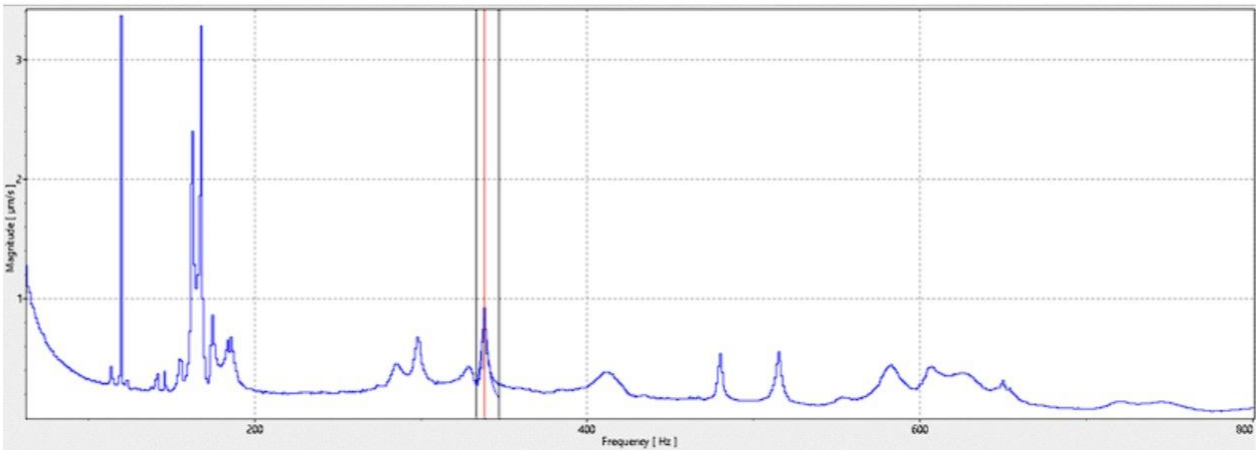

*Figure 7: Magnitude of vibration (*µm/s*) for each frequency from 1 Hz – 800 Hz for the FFF*

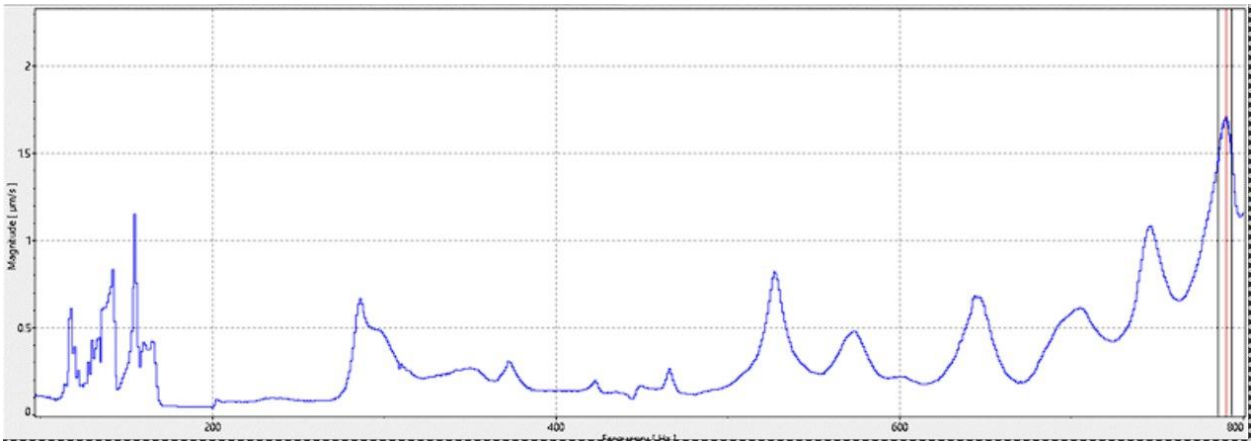

Figure 8: Magnitude of vibration (µm/s) for each frequency from 1 Hz – 800 Hz for the HFF

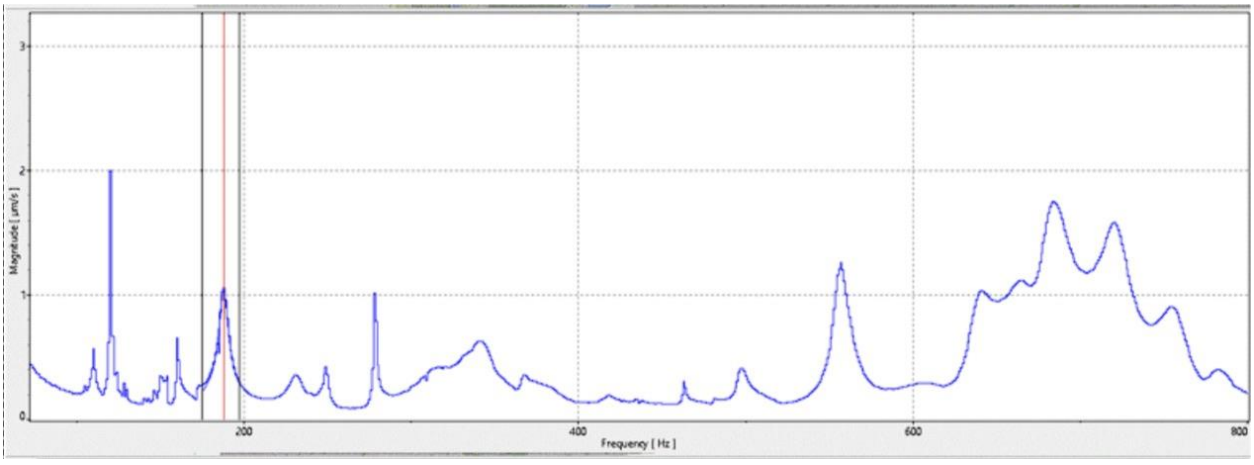

*Figure 9: Magnitude of vibration (*µm/s*) for each frequency from 1 Hz – 800 Hz for the UFF*

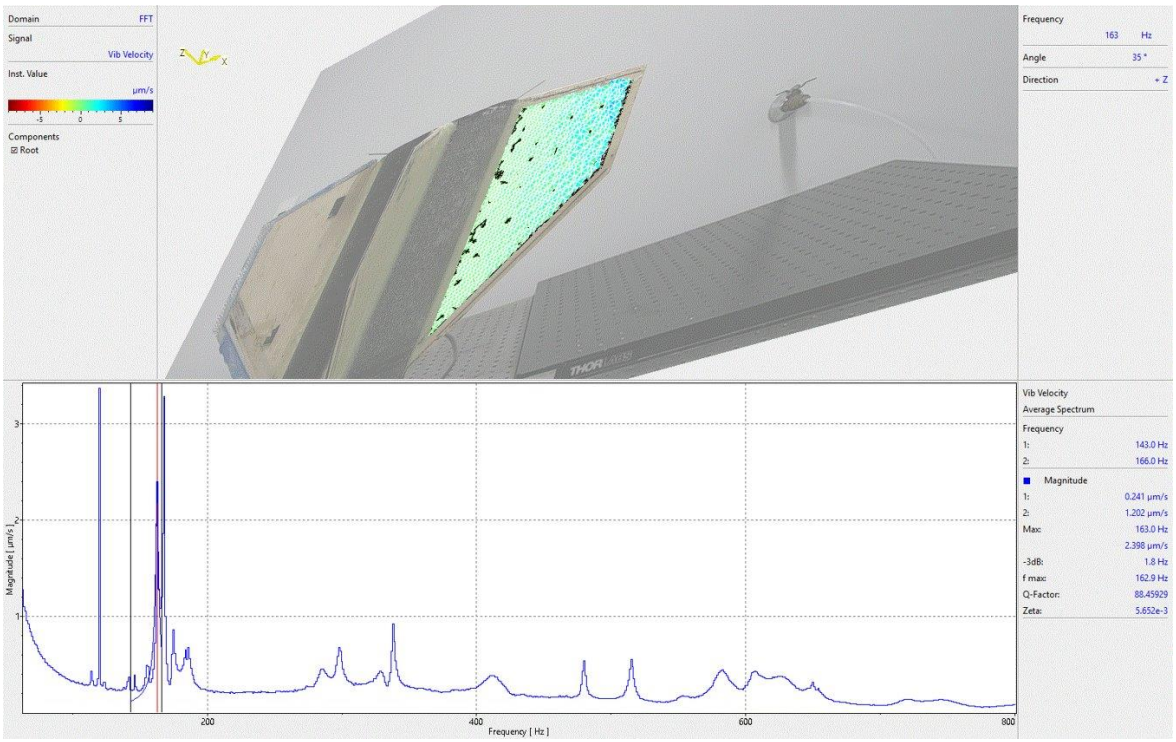

Figure 10: Fin animation at the first bending mode at 162.9 Hz (Only animates in .docx)

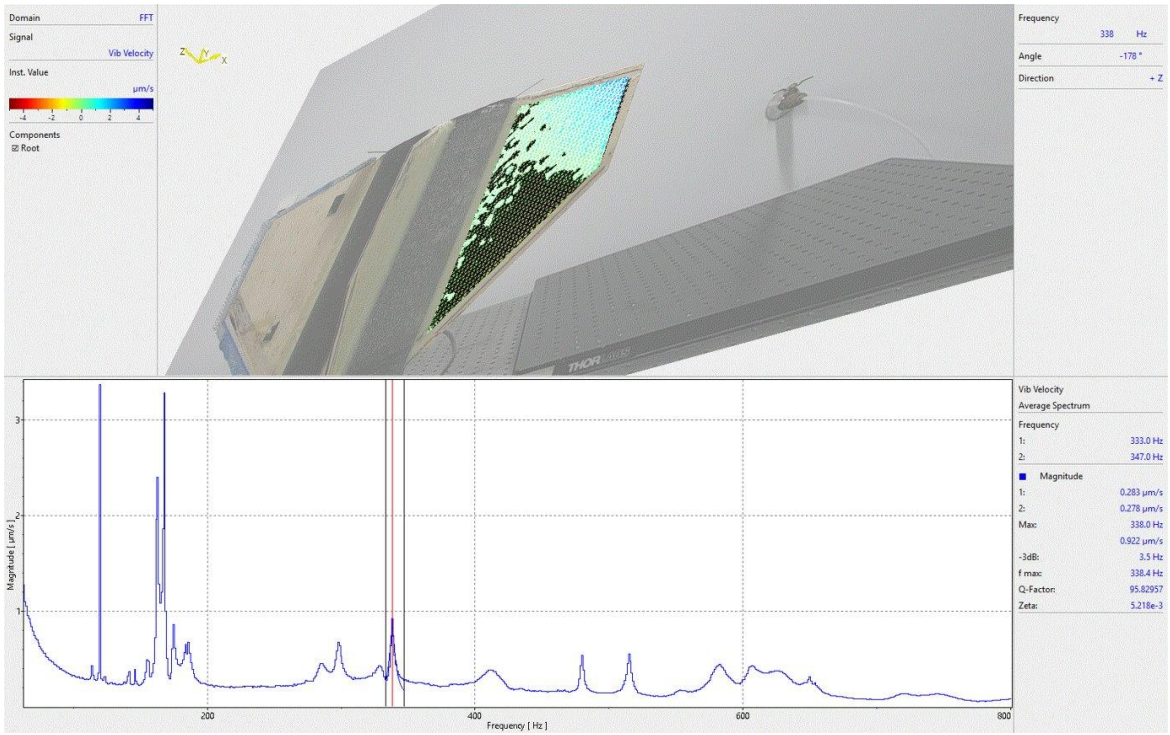

Figure 11: Fin animation at the first torsional mode at 338 Hz (Only animates in .docx)

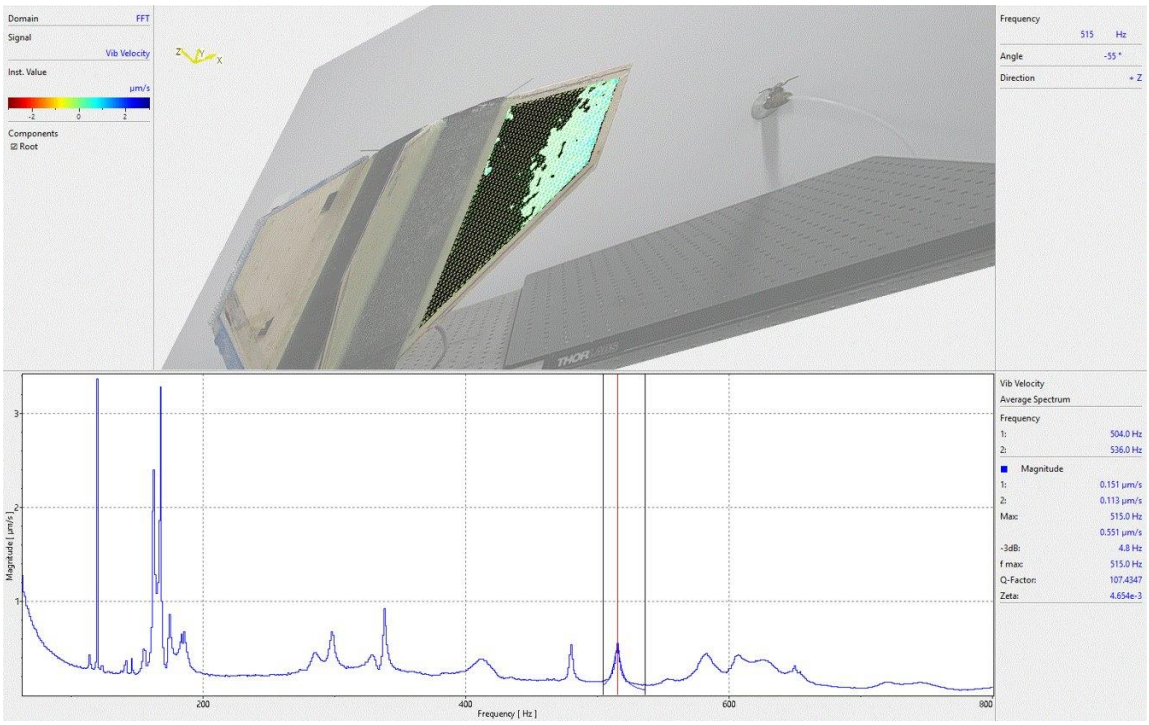

Figure 12: Fin animation at the second bending mode at 515 Hz (Only animates in .docx)

As we visually understand what the first bending, second bending, and tortional modes look like, we can identify the frequencies in which they occur each occur for the three fin types. This data is shown and explored further in the results section.

3.4 Ansys Simulation

Additionally, we decided that a simulation in Ansys would be useful to compare against our real-world data. Below, figures 12, 13, and 14 show the simulated first bending, first torsional, and second bending modes of a fully fiberglass fin at 170Hz, 482 Hz, and 951 Hz respectively. An additional simulation of a fully wood fin was also conducted. *These simulations will allow a comparison to our measured values and show how accurate or inaccurate these simulations are.*

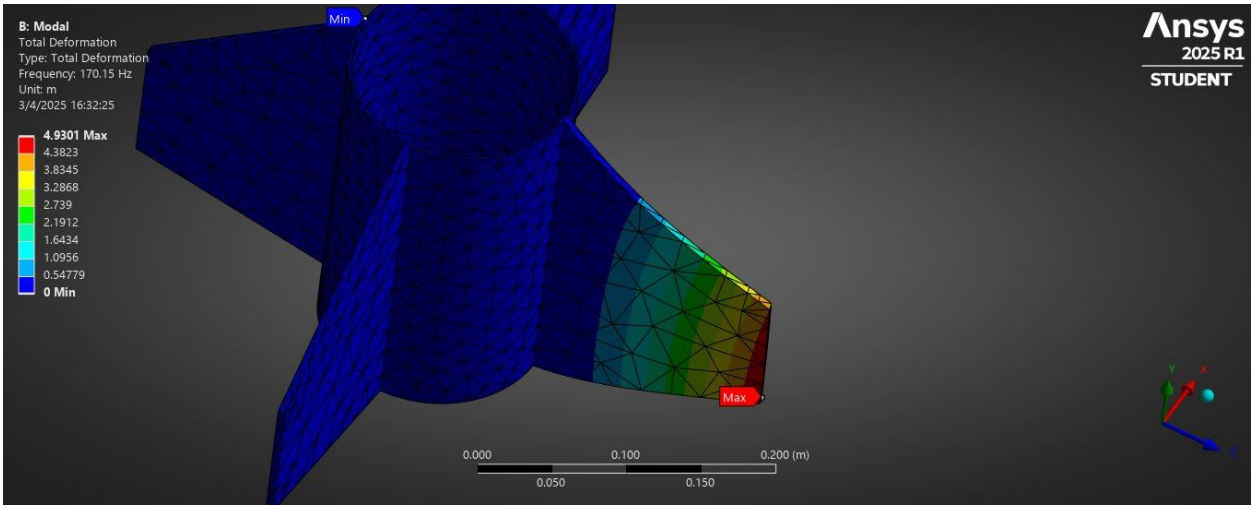

Figure 13: Ansys simulation of fiberglass fin at the first bending mode at 170 Hz

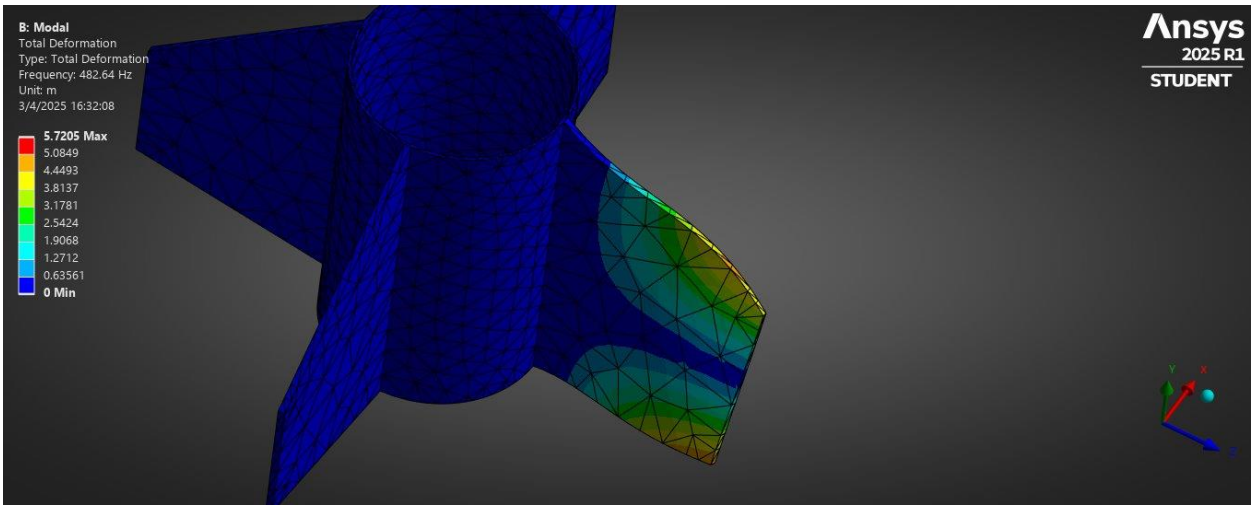

Figure 14: Ansys simulation of fiberglass fin at the first torsional mode at 482 Hz

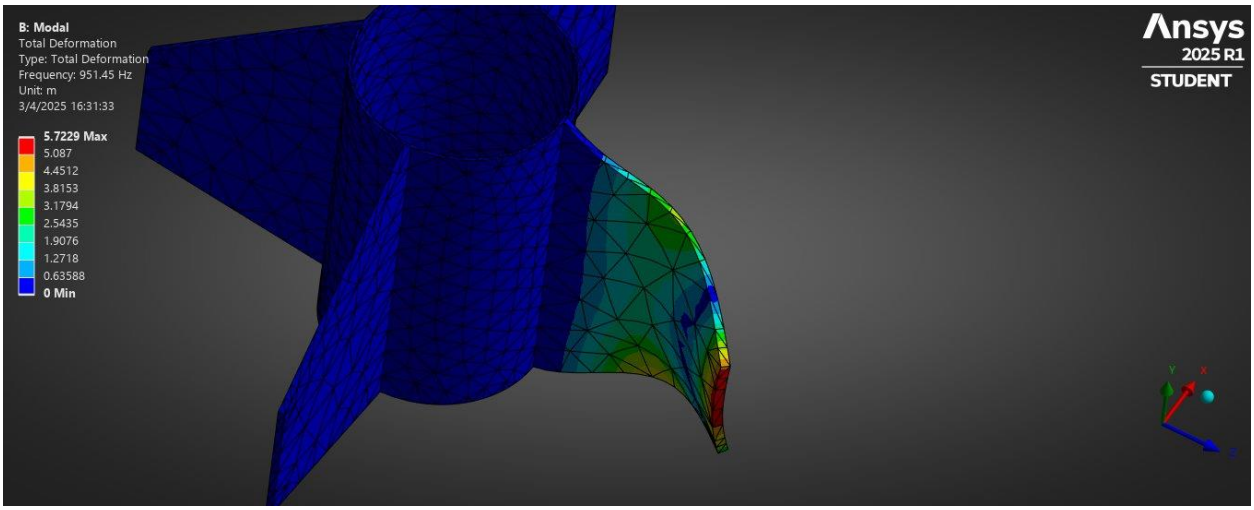

Figure 15: Ansys simulation of fiberglass fin at the second bending mode at 951 Hz

4.0 Results and Discussion

We gathered data from 3 different real fins and 2 different simulated fins. The real fins will be referred to as Fully Finished Fin (FFF), Half Finished Fin (HFF), and Unfinished Fin (UFF). The FFF is a ~3mm plywood fin with 3 layers of fiberglass totaling ~1mm on each side. Both the HFF and UFF are ~3mm plywood fins with 3 layers of fiberglass on only one side. The two simulated fins were computed in ANSYS and are referred to as Simulated Fiberglass Fin (SIM FG) and Simulated Wood Fin (SIM WOOD). ANSYS workbench was used to calculate the natural frequencies of the simulated fins, and the PSV-500 SLDV was used to calculate the natural frequencies of the real fins. Values of ω_h and ω_α are tabulated in table 1 below. For the HFF and UFF, no first order bending frequency could be found, so a low frequency second order bending mode was substituted.

Fin Name	ω_h	ω_α	$\frac{\omega_h}{\omega_\alpha}$
FFF	$1067\ rad/s$	$2213\ rad/s$	0.482
HFF	$1181\ rad/s$	$1451\ rad/s$	0.814
UFF	$973\ rad/s$	$1796\ rad/s$	0.542
SIM FG	$1069\ rad/s$	$3028\ rad/s$	0.353
SIM WOOD	$1457\ rad/s$	$3895\ rad/s$	0.374

Table 1: First bending, first torsional, and the ratio between them for the three measured fins and the two simulations

As mentioned in the methods section, we have approximated values of $\kappa \approx \frac{1}{5}$, $a \approx -0.4$ and $x_a \approx 0.3$ for the fins in question. Using this as well as the above ratios, it is possible to calculate the fin flutter frequency. As shown in figure 15 below, the values of $\frac{\omega_f}{\omega_\alpha}$ were found visually using the graph from TN 685. This yields $\frac{\omega_h}{\omega_\alpha}$ values shown in Table 2 below.

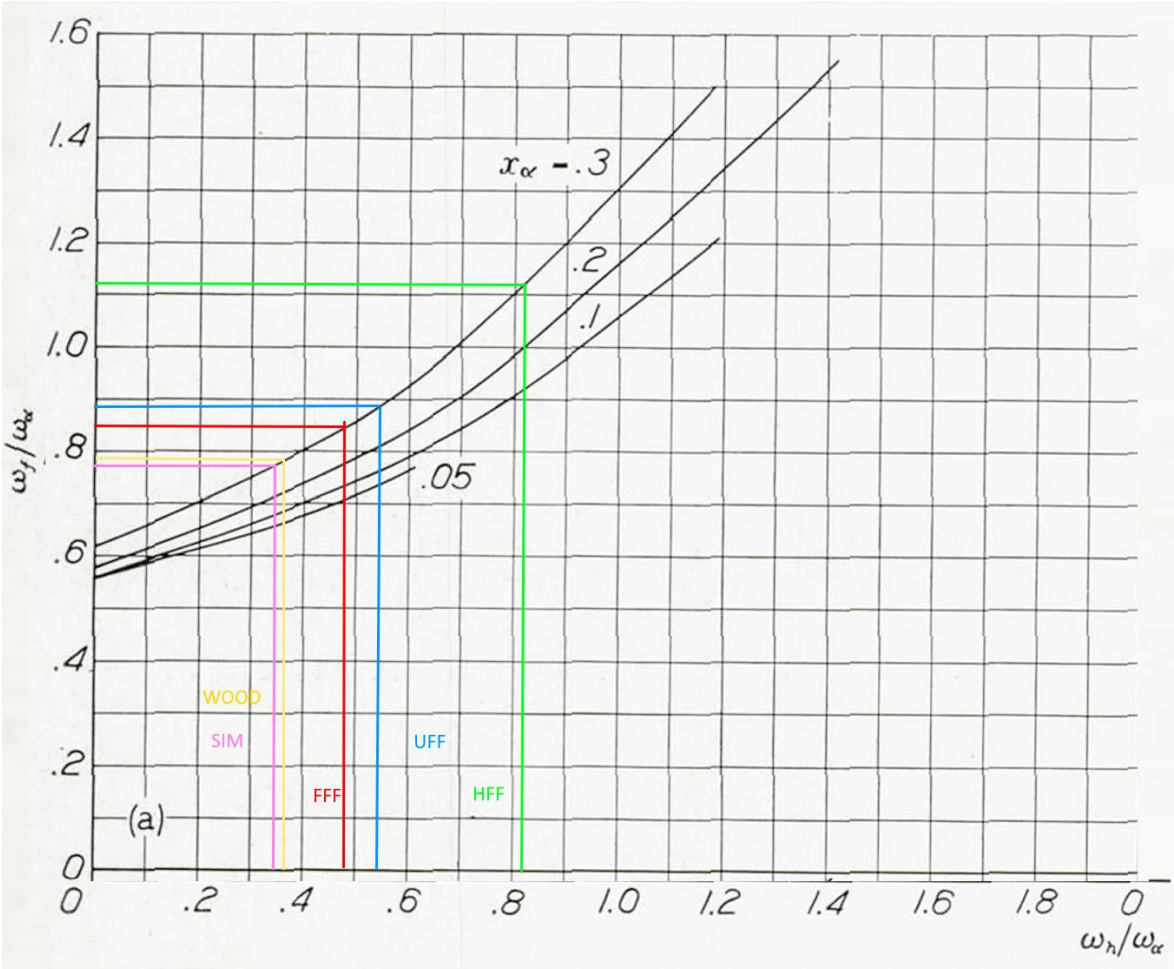

Figure 16: Graph a in figure 2 with visual illustration on how table 2 was filled

Fin Name	$\frac{\omega_f}{\omega_\alpha}$	$\frac{\omega_f}{2 * pi}$
FFF	0.85	287Hz
HFF	1.11	256Hz
UFF	0.89	254Hz
SIM FG	0.77	371Hz
SIM WOOD	0.79	489Hz

Table 2: Ratio of flutter frequency to first torsional frequency and the flutter frequency for each measured and simulated fin

An interesting trend that can be seen here is that though the FFT spectra for the HFF and UFF are very different, they have almost the exact same flutter frequency. This makes sense because they are physically very similar, despite having different resonance characteristics. These values can be used to solve for the flutter velocity using the equations below.

$$X = \frac{{r_\alpha}^2}{\kappa} * \left(\frac{\omega_\alpha}{\omega}\right)^2 \quad (6)$$

$$v = \frac{r_\alpha \omega_\alpha b}{\sqrt{\kappa}} * \frac{1}{k} * \frac{1}{\sqrt{X}} \quad (7)$$

In these equations, v is the flutter velocity, and is what is being solved for. The variable r_α is the radius of gyration about the aerodynamic center (center of pressure), and is assumed to be equal to ¼. The value of b is equal to half of the total chord length, or 5 inches. It is calculated that κ approximately equal to ¼. After consulting the paper on the subject, k is assumed to be 0.8, as it is asserted to be commonly close to 1, and is lower with reduced wing span. Using these equations, the following flutter speeds were calculated and displayed in table 3.

Fin Name	v_f
FFF	940 ft/s
HFF	839 ft/s
UFF	832 ft/s
SIM FG	1214 ft/s
SIM WOOD	1602 ft/s

Table 3: Flutter velocity for each measured and simulated fin

Several expected trends can be seen in this data. The flutter velocity for the HFF and UFF are very similar to each other because of the aforementioned geometrical similarity of these fins. The values for both UFF and HFF are lower than that for FFF, which makes sense because they are not only thinner but have less fiberglass on them. The value for SIM FG is higher than that for FFF because it is making the assumption that the entire fin is fiberglass, when in reality only the skin is. The SIM WOOD value is higher than FFF because it's assuming that the wood involved is oak hardwood instead of the pine plywood that's actually being used.

The final step is to compare this to the value obtained by using the NACA TN 4197 algorithm [1]. A spreadsheet was used to tabulate this value, shown in figure 16 below.

Fin Geometry:	Tapered Swept Rect.	G10 Fiberglass	1/4" thickness	1.5 mm Epoxy Layer		
Root Chord (Cr)	0.254	m		Speed of Sound (a)	332.5823	m/s
Tip Chord (Ct)	0.1016	m		Temperature (Tc)	2	C
Thickness (t)	0.00735	m		P/Po	0.784552	
Thickess Ratio (t/Cr)	0.028937008			Altitude	2000	m
Semi-Span Length (l)	0.1524	m				
				Flutter Velocity (Vf)	326.176	m/s
Aspect Ratio (A)	0.857142857				1043.763	ft/s
Area	0.02709672	m^2				
Taper Ratio (Lamda)	0.4					
Shear Modulus	1,300,000	Kpa				

Figure 16: Spreadsheet to calculate the flutter velocity as per NACA TN 4197 [1]

The calculated value of $v_f = 1044\ ft/s$ is very close to both the 940 of the FFF and the 1214 of the SIM FG fin. This proves that the algorithm given in NACA TN 4197 is valid even in the case of composite fins. This allows future analysis to use the simplified NACA TN 4197 algorithm instead of requiring computationally intensive finite element simulations.

5.0 Conclusions and Future Work

This study successfully proved the validity of the NACA-4197 algorithm in predicting fin flutter. Especially as this algorithm was not designed for the fiberglass composite fins that were used for our measurements. Additionally, this study also proved the difficulty in simulating these composite fins. The simulated values we gathered were quite far off of the measured values. Although this is due to using pure fiberglass and pure wood fins in our simulations rather than the fiberglass composite and wood core of our measured fins. This shows the difficulty in simulating these fins to find data like ours and reinforces the need for measuring each fin.

Future work should involve:

- Expanding the study to include additional composite materials with varying fiber orientations
- Conducting wind tunnel testing to validate results under dynamic flight conditions
- Refining computational simulations to incorporate more detailed material properties and boundary conditions

These steps will provide further validation of the NACA-4197 model and ensure its usefulness in practical aerospace applications.

OBJ

6.0 References

[1] D. J. Martin, "SUMMARY OF FLUTTER EXPERIENCES AS A GUIDE TO THE PRElIMINARY DESIGN OF LIFTING SURFACES ON MISSILES," Langley Aeronautical Laboratory, Langley Field, 1958

[2] H. Tabatabai, D. E. Oliver, J. W. Rohrbaugh, and C. Papadopoulos, “Novel Applications of Laser Doppler Vibration Measurements to Medical Imaging,” Sensing and Imaging: An International Journal, vol. 14, no. 1–2, pp. 13–28, Jun. 2013, doi: https://doi.org/10.1007/s11220-013-0077-1.

[3] T. THEODORSEN and I. E. GARRICK, "MECHANISM OF FLUTTER A THEORETICAL AND EXPERIMENTAL INVESTIGATION OF THE FLUTTER PROBLEM," NATIONAL TECHNICAL INFORMATION SERVICE, Springfield, 1940.